Available online at www.sciencedirect.com
SCIENCE DIRECT
Intermetallics 13 (2005) 764–769
Intermetallics
www.elsevier.com/locate/intermet

Mechanical behavior of $Fe_{65.5}Cr_4Mo_4Ga_4P_{12}C_5B_{5.5}$ bulk metallic glass

M. Stoica[a,*], J. Eckert[a,b], S. Roth[a], Z.F. Zhang[c], L. Schultz[a], W.H. Wang[d]

[a]*Leibniz Institute for Solid State and Materials Research Dresden, Institute of Metallic Materials, P.O. Box 270016, D-01171 Dresden, Germany*
[b]*Physical Metallurgy Division, Department of Materials and Geo Sciences, Darmstadt University of Technology, Petersenstraße 23, D-64287 Darmstadt, Germany*
[c]*Shenyang National Laboratory for Materials Science, Institute of Metal Research, Chinese Academy of Sciences, 110016 Shenyang, People's Republic of China*
[d]*Institute of Physics, Chinese Academy of Sciences, P.O. Box 603, 100080 Beijing, People's Republic of China*

Received 14 October 2004; received in revised form 2 December 2004; accepted 2 December 2004

Abstract

$Fe_{65.5}Cr_4Mo_4Ga_4P_{12}C_5B_{5.5}$ bulk amorphous rectangular bars with a cross-section of 2×2 mm^2 and a length of 30 mm were produced by copper mold casting. The as-cast bars as well as annealed samples were investigated by compression and Vickers hardness tests. The fracture strength for the as-cast samples σ_f is 2.8 GPa and the fracture strain ε_f is 1.9%. Upon annealing at 715 K for 10 min, i.e. at a temperature below the calorimetric glass transition, the fracture strain drops to 1.6% and no plastic deformation is observed. The Vickers hardness *HV* for the as-cast samples is about 885, and increases to 902 upon annealing. The fracture behavior of this Fe-based bulk glassy alloy is significantly different in comparison with the well-studied Zr-, Cu- or Ti-based good glass-formers. The fracture is not propagating along a well-defined direction and the fractured surface looks irregular. Instead of veins, the glassy alloy develops a high number of microcracks.

Keywords: B. Glasses, metallic; B. Fracture stress; F. Mechanical testing

1. Introduction

Multicomponent alloys with high glass-forming ability and a wide supercooled liquid region between the glass transition temperature T_g and the crystallization temperature T_x give promise to expand the application field of iron-base amorphous alloys as soft magnetic materials [1]. Because of the absence of crystalline anisotropy, the $Fe_{65.5}Cr_4Mo_4Ga_4P_{12}C_5B_{5.5}$ amorphous alloy exhibits good soft magnetic properties, characterized by a low coercive force and a high permeability [2]. The presence of Cr and Mo in the composition not only improves the glass-forming ability, but also increases the corrosion resistance of the material in comparison with conventional steels used for magnetic applications [3,4]. Besides the good soft magnetic properties, such alloys also require good mechanical strength for possible use in magnetic devices as magnetic sensors, magnetic valves or magnetic clutches.

However, despite an increasing number of published papers about the mechanical properties of bulk metallic glasses (BMG), most of these reports deal only with non-ferrous Zr-, Ti- or Cu-based [5–7]. The mechanical properties of bulk Fe-based glasses started to be investigated only in the past few years [8–12]. One reason is the difficulty to cast such ferrous glasses in bulk form, because of their relatively low glass-forming ability. The maximum achievable diameter for soft magnetic Fe-based BMGs is limited to about 3–4 mm. This is in contrast to Zr- or Cu-based glassy alloys, which can easily reach even 10 mm diameter [7]. This is because the critical cooling rate necessary for amorphization in the case of soft magnetic Fe-based alloys is 10^2–10^3 K/s, whereas for Zr- or Cu-based metallic glasses, the required critical cooling rate is only 10^0–10^2 K/s [7], i.e. at least one order of magnitude lower than that for the Fe-based BMGs. Only very recently, Ponnambalam et al. [11] and, independently, Lu et al. [12] succeeded to cast Fe-based BMGs with a thickness larger than one centimeter (using some small addition of Y,

* Corresponding author. Tel.: +49 351 4659 253; fax: +49 351 4659 541.
E-mail address: m.stoica@ifw-dresden.de (M. Stoica).

0966-9795/$ - see front matter © 2005 Elsevier Ltd. All rights reserved.
doi:10.1016/j.intermet.2004.12.016

Ln and/or Er), but their glasses are paramagnetic at room temperature, with a Curie temperature of around 55 K.

The known strength values for non-ferrous glassy alloys are in the range of: 1.5–1.8 GPa for Zr-based alloys, 1.7–1.9 GPa for Ti-based alloys, 1.9–2.5 GPa for Cu-based alloys or 2.7–3.1 GPa for Ni-based alloys (for an overview, see [9]). For our $Fe_{65.5}Cr_4Mo_4Ga_4P_{12}C_5B_{5.5}$ BMG, the fracture strength exceeds 2.8 GPa. In the case of Zr- or Cu-based bulk glassy alloys, the fracture usually proceeds along a shear plane, which is declined by $\sim 45^\circ$ to the direction of the applied load, and the fracture surface exhibits a well-developed vein pattern [6,7]. In contrast, the studied $Fe_{65.5}Cr_4Mo_4Ga_4P_{12}C_5B_{5.5}$ samples develop a cleavage-like fracture surface with a high number of microcracks, which finally destroy the sample completely. The fracture surface appears to contain a high number of small fracture zones, which are probably generated at the same time due to the very high stress level upon deformation.

The aim of this work is to present results obtained from compression and indentation tests of bulk glassy $Fe_{65.5}Cr_4Mo_4Ga_4P_{12}C_5B_{5.5}$ as-cast specimens and samples subjected to structural relaxation below the calorimetric glass transition temperature, as well as a comparison with other data available in the literature.

2. Experimental details

Bulk glassy 30 mm long rectangular bars with a cross section of 2×2 mm^2 were prepared from a master alloy with nominal composition $Fe_{65.5}Cr_4Mo_4Ga_4P_{12}C_5B_{5.5}$ starting from the pure elements with purity better than 99.9%. The samples were obtained by induction melting and injection of the melt into a copper mold. The thermal stability was investigated by differential scanning calorimetry (DSC) using a Netzsch DSC 404 under a flow of purified argon. The glass transition temperature T_g and the crystallization temperature T_x were determined as the onset temperatures of the glass transition and the crystallization events, respectively, during heating with a constant rate of 20 K/min. In addition, the melting temperature T_m defined by the liquidus temperature T_{liq} at the onset of solidification upon cooling with a constant rate of 20 K/min was measured using the same Netsch DSC 404 calorimeter. The amorphous structure as well as the crystallization behavior and the magnetic properties of these glassy samples have already been investigated and published previously [13–15].

In order to investigate the mechanical behavior, different techniques were used. First, room temperature compression tests using an electromechanical Instron 8562 testing device were performed for as-cast and annealed 2×2 mm^2 rectangular bars. The length of the samples was between 4 and 5 mm and the machine was operated in the constant position rate mode, with a displacement of 10^{-3} mm/s. The corresponding strain rate was evaluated as 10^{-4} s^{-1}. From the compression tests, the fracture strength σ_f, the fracture strain ε_f, the yield strength σ_y, the yield strain ε_y and the Young's modulus E were derived.

The Vickers hardness was measured for the same kind of bar samples using a computer controlled Struers Duramin 5 hardness tester. The tests were performed using a typical diamond indenter in the form of pyramid with square base and an angle of 136° between opposite faces applying a load of 1.96 N for 10 s. The diagonal of the imprints as well as the hardness were calculated using a Digital Video Measuring System. For the indentations, the samples were embedded in epoxy resin and the measured surface was carefully polished with a paste containing diamond particles with a diameter smaller than 0.25 μm.

The characteristics of the fractured surface as well as the features of the indents after the hardness tests were studied by scanning electron microscopy (SEM), using a JEOL JSM 6400 microscope operated at 25 kV.

3. Results

Fig. 1 shows a typical DSC scan recorded using a constant heating rate of 20 K/min for an $Fe_{65.5}Cr_4Mo_4Ga_4\ P_{12}C_5B_{5.5}$ as-cast rectangular bar, starting from room temperature, all the way up through melting and overheating up to 1573 K, as well as the signal obtained upon cooling at the same rate down to 1073 K. Upon heating to 1073 K, the DSC scans reveals a glass transition followed by a supercooled liquid region and crystallization. Further on, the alloy is melted, overheated and subsequently cooled. The main characteristic temperatures are $T_g=745$ K, $T_x=806$ K, and $T_m=1322$ K. The values of the extension of the supercooled liquid region $\Delta T_x=T_x-T_g$ of 61 K, as well as of the reduced glass transition temperature $T_{rg}=T_g/T_m$ of 0.56 are characteristic for an alloy with good glass-forming ability and good thermal stability against crystallization [7].

Fig. 2 shows the compressive stress-strain curves for as-cast and annealed rectangular bars. The annealing

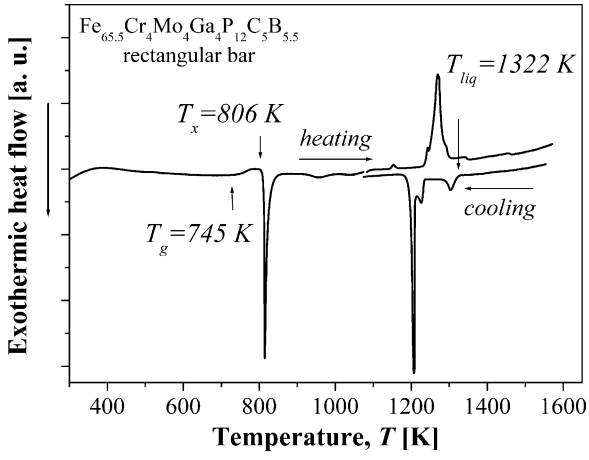

Fig. 1. The DSC scans at 20 K/min for $Fe_{65.5}Cr_4Mo_4Ga_4P_{12}C_5B_{5.5}$ as-cast rectangular bar.

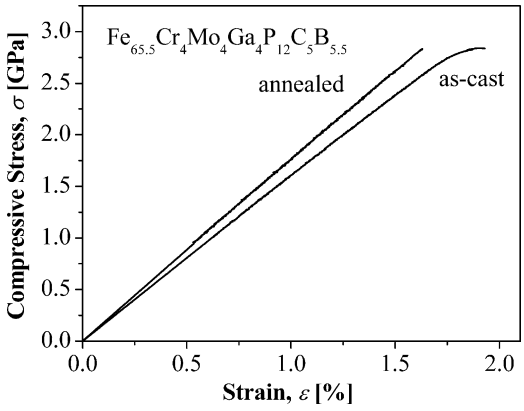

Fig. 2. Compressive stress-strain curves for $Fe_{65.5}Cr_4Mo_4Ga_4P_{12}C_5B_{5.5}$ as-cast and annealed rectangular bars.

was done for 10 min at 715 K, i.e. at a temperature equal to $T_g - 30$ K, using a heating and cooling rate of 5 K/min. It can be noted that the fracture stress retains almost the same value after annealing, but the sample becomes more brittle and no plastic deformation is observed.

The yield strength σ_y defined by the stress corresponding to an offset strain of 0.1% is 2.82 and 2.84 GPa for the as-cast and for the annealed sample, respectively. The corresponding compressive yield strain ε_y is 1.76 and 1.60%, respectively. The Young's modulus E is 161 GPa for the as-cast state and 177 GPa after annealing. The fracture of both samples occurs at nearly the same value of compressive stress ($\sigma_f \sim 2.82$–2.84 GPa), but the corresponding fracture strain ε_f is different: 1.91% for the as-cast sample and 1.63% for the annealed one. The as-cast sample shows a small plastic deformation ε_{pl} of 0.15%, but in the case of the annealed bar the plastic regime extends only over 0.03%.

Concerning the hardness measurements, 20 indents were performed in each sample in order to have an accurate result. For the as-cast bars, the average value is $HV = 885$ (8.68 GPa) with a typical standard deviation of 5. The hardness of the annealed bars increases up to $HV = 902$ (8.84 GPa) with a standard deviation of 2.1. The smaller value of the standard deviation in the case of the annealed samples indicates a more homogeneous behavior of the annealed specimens in comparison with the as-cast state. Fig. 3 shows an SEM micrograph of the surface of an as-cast sample with the mark of an indent. The slips generated by the Vickers diamond indenter and the absence of any visible crack can be easily observed. These features are in accordance with the behavior found from the compression test.

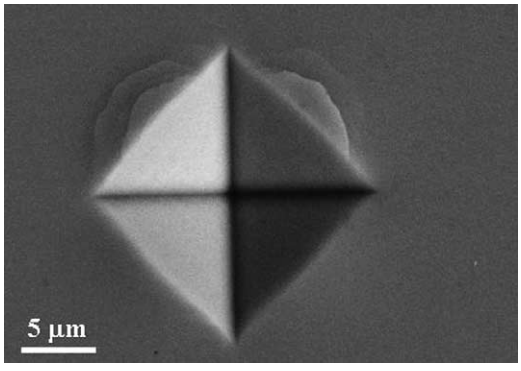

Fig. 3. SEM micrograph (topological view) showing the surface of as-cast investigated sample with a mark of an indent. It is possible to observe the slips generated by the Vickers diamond indenter.

4. Discussion

In the compression tests, both the as-cast and the annealed samples exhibit a purely elastic deformation up to certain values of the applied stress, followed by a plastic deformation, which is readily apparent in the case of the as-cast bars but very small in the case of annealed material. The samples remain macroscopically intact up to a high level of applied stress. Table 1 summarizes the deformation data obtained from the compression tests, together with some literature values for other Fe- or Fe–Co-base bulk glassy alloys. For our samples, the offset yield is around 3 GPa, and the corresponding strain is between 1.6 and 2%. The value of Young's modulus for the annealed $Fe_{65.5}Cr_4Mo_4Ga_4P_{12}C_5B_{5.5}$ 2×2 mm^2 bar is 177 GPa, thus being higher than for the as-cast sample (161 GPa). Upon structural relaxation, as induced by the annealing below T_g, the packing density of the glass increases slightly [16]. The mechanical properties follow the same trend, i.e. the Young's modulus increases and the plasticity drops (i.e. the brittleness of these glassy samples increases upon annealing).

The values are comparable with the data reported by Inoue et al. [8] for $(Fe_{0.75}B_{0.15}Si_{0.1})_{96}Nb_4$ or $Fe_{77}Ga_3P_{9.5}C_4B_4Si_{2.5}$ glassy rods with 1.5 and 2 mm diameter, respectively. For another ferromagnetic alloy, cast iron (FC20) with 0.4 wt.% boron, a fracture strength of 3.48 GPa has been reported [10], but the Young's modulus is only 125 GPa. Upon annealing this alloy for 1 h at 1200 K, i.e. upon precipitation of some FeC particles, the fracture strength decreases to 1.53 GPa, less than half in comparison with the initial value, but the plastic strain extends over 9% [10]. It must be mentioned that the values corresponding to annealed samples were measured upon tensile testing a rod of 0.5 mm diameter. The highest strength value reported up to now for a bulk glassy ferromagnetic alloy is 5.185 GPa as measured for a 2 mm diameter as-cast rod of composition $Co_{43}Fe_{20}Ta_{5.5}B_{31.5}$ [9]. The Young's modulus is 268 GPa and no plastic deformation at room temperature was noticed. At 698 K, a temperature 212 K below the glass transition temperature, the compressive fracture strength increases slightly to 5.334 GPa.

The values of the strength are much higher than the known values for non-ferrous glassy alloys: 1.5–1.8 GPa for Zr-based alloys, 1.7–1.9 GPa for Ti-based alloys, 1.9–2.5 GPa for Cu-based alloys or 2.7–3.1 GPa for Ni-based alloys (these values are summarized in [9]). In the case when our samples show plastic deformation, it is

Table 1
The values of yield stress σ_y, yield strain ε_y, fracture stress σ_f, fracture strain ε_f, the pure plastic deformation strain ε_{pl}, Young's modulus E and Vickers hardness for the analysed samples, as well as the available data from literature

Type and composition	σ_y (GPa)	ε_y (%)	σ_f (GPa)	ε_f (%)	ε_{pl} (%)	E (GPa)	HV
Bar 2×2 mm as-cast $Fe_{65.5}Cr_4Mo_4Ga_4P_{12}C_5B_{5.5}$	2.82	1.76	2.84	1.91	0.15	161	885
Bar 2×2 mm annealed $Fe_{65.5}Cr_4Mo_4Ga_4P_{12}C_5B_{5.5}$	2.84	1.60	2.84	1.63	0.03	177	902
Rod ϕ 1.5 mm as-cast $(Fe_{0.75}B_{0.15}Si_{0.1})_{96}Nb_4$ [8]	3.16	1.8	3.250	2.2	0.4	175	1060
Rod ϕ 2 mm as-cast $Fe_{77}Ga_3P_{9.5}C_4B_4Si_{2.5}$ [8]	2.98	1.9	3.16	2.2	0.3	182	870
Rod ϕ 2 mm as-cast $Co_{43}Fe_{20}Ta_{5.5}B_{31.5}$ [9]	5.18	0.02	5.185	0.02		268	
Rod ϕ 2 mm annealed $Co_{43}Fe_{20}Ta_{5.5}B_{31.5}$ [9]	5.33	0.02		0.03	0.01	268	
Rod ϕ 2 mm as-cast FC20+0.4 wt.% B [10]			3.48			125	970
Rod ϕ 0.5 mm annealed FC20+0.4 wt.% B [10]	1.42		1.53		9		1120
Rod ϕ 12 mm $Fe_{48}Cr_{15}Mo_{14}Er_2C_{15}B_6$ [11]	~4					200	~1200
Rod ϕ 12 mm $(Fe_{44.3}Cr_5Co_5Mo_{12.8}Mn_{11.2}C_{15.8}B_{5.9})_{98.5}Y_{1.5}$ [12]	~3					257	1224

around 0.15% and this plastic behavior should be also noted, because usually the crystalline soft magnetic materials used for magnetic devices are brittle [17].

The appearance of the fracture surface was investigated by SEM. Fig. 4(a–c) show micrographs of an as-cast rectangular bar after fracture at different magnifications. First, it is noticed that the cross-sectional dimensions are not altered upon compression (Fig. 4(a)). Another feature is the appearance of the fracture surface (Fig. 4(b) and (c)). The observed fracture behavior is totally different from that observed for Zr- or Cu-based bulk glassy alloys. For Zr-based metallic glasses, it is previously considered that the compressive fracture usually proceeds along a shear plane inclined by 45° to the loading axis [18]. However, recent systematic investigation on the glasses with different alloy systems indicates that the shear fracture always deviates from the maximum shear stress plane either under compression or under tension [19]. For our samples, the fracture surface appears to consist of a high number of small fracture zones, which leads to breaking of the samples into many small parts, as indicated in Fig. 4(a–c). This agrees well with the Ti-based composites containing dendrites [20,21]. It indicates that the fracture of metallic glasses can occur either in a shear mode or in a break mode, depending on the constituent elements and microstructure in detail. The actual failure mode of a metallic glassy sample is a competition result between shear fracture and distensile fracture as reported by Zhang et al. [20]. For the Fe-based glasses, it has quite high fracture strength, indicating that the critical shear fracture stress must be high enough in comparison with the bonding force among the constituent elements in the present glass. The brittleness can be also enhanced by presence of metalloids, i.e. C, B and P [16]. Inoue and co-workers [8] supposed that such cracks as presented in Fig. 4(c) are relatively easy to be initiated nearly simultaneously because the stress level is very high, around 3 GPa, and the shock wave caused by initiation of one crack induces the generation of other cracks at different sites.

The similarities of fracture behavior between our samples and Ti-based composites may also indicate that the Fe-based BMG contains a small volume fraction of (nano)crystals. The possible existence of a small volume fraction of (nano)crystalline precipitates, which may be present in the glassy matrix, is difficult to be ruled out by means of classical X-ray diffraction or by DSC [14]. A suitable method is the X-ray diffraction in transmission configuration, using a high intensity high-energy monochromatic synchrotron beam [14], an investigation which was not performed for present Fe-based BMG. Thus, whether the samples contain or not small volume fraction of crystalline inclusions remains an open question.

Fig. 5 summarizes the relationship between σ_f and T_g for a number of bulk glassy alloys, as given in the literature [8]. Our results are illustrated by the open circle. Despite some scatter, all data for Fe-based bulk glassy alloys appear to lie in the same region. Considering that T_g reflects the bonding nature between the constituent elements [22], the high strength of the Fe-based bulk glassy alloys seems to originate from the high bonding forces between the constituent elements. The rather good linear relation shown in Fig. 5 should indicates the absence of difference in the mechanical properties between metal-metalloid-type glassy alloys and simple metal type alloys or transition metal-type alloys. The fracture surface of our investigated samples is without shear plane and vein pattern because such cleavage-like fracture usually does not go along a shear plane but frequently forms a rugged

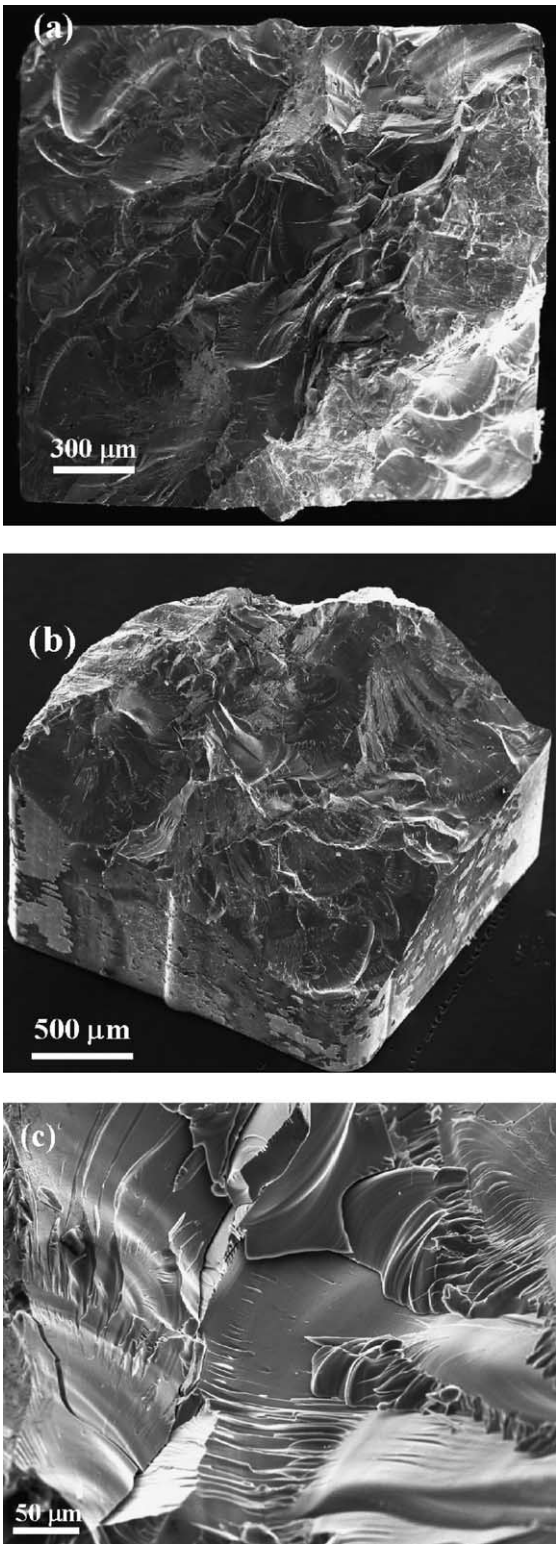

Fig. 4. SEM micrograph (topological view) showing the fracture surface after compression test: (a) general overview, (b) side view and (c) detail at higher magnification.

fracture surface or breaks into pieces. Since the shear stress does not work significantly in the fracture, the vein-like feature (produced under high shear stress) will not appear.

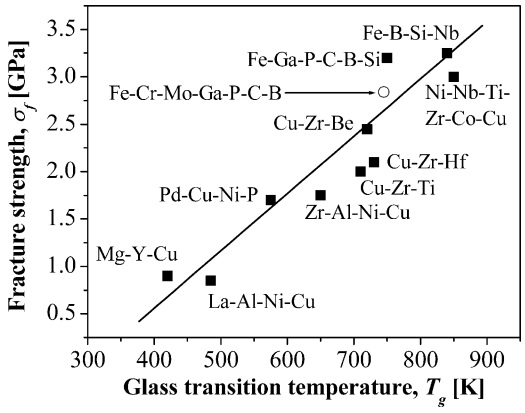

Fig. 5. Relationship between compressive fracture strength σ_f and glass transition temperature T_g from literature [8]. Our results are illustrated by the open circle.

The ratio σ_f/E attains values of around 0.017 and $H_v/3E$ takes values of 0.018 and 0.016 for the as-cast and annealed samples, respectively. Hence, the relationship between the fracture strength and the hardness $\sigma_f \approx H_v/3$ is verified [16]. Considering that a number of amorphous alloys reported up to date have nearly fixed values of about 0.02 for σ_f/E and $H_v/3E$ [16], it is concluded that the studied Fe-based bulk glassy alloys follow the same trend. The agreement also suggests that the Fe-based bulk glassy alloys have an elastic-plastic deformation mode similar as other non-ferrous bulk glassy alloys. The main differences are a much higher strength level, which can be achieved upon compression tests, and the different mechanism of fracture.

5. Summary

The bulk amorphous Fe-based alloy with the nominal composition $Fe_{65.5}Cr_4Mo_4Ga_4P_{12}C_5B_{5.5}$ obtained by copper mold casting exhibits at room temperature a high strength and some compressive plastic strain. An annealing/structural relaxation treatment at elevated temperature does not affect the stress level, which remains almost the same, but the plasticity disappears. The fracture mechanism is different in our Fe-based bulk glassy alloy in comparison with other non-magnetic metallic glasses. The actual failure mode of metallic glassy sample is a competition result between shear fracture and distensile fracture.

Acknowledgements

The authors thank H. Klauß and Dr A. Güth for their help with compression tests and SEM investigations, and S. Kuszinski, H. Schulze and S. Müller-Litvanyi for technical assistance. Partial financial support from the German Science Foundation under grant number Ec 111/12-1 and from the EU within the framework of the RTN-networks on bulk metallic glasses (HPRN-CT-2000-00033) and ductile

BMG composites (MRTN-CT-2003-504692) is also acknowledged.

References

[1] Roth S, Ferchmin AR, Kobe S. In: H.P.J. Wijn, editor. Landolt-Börnstein: numerical data and functional relationships in science and technology. Magnetic properties of metals, vol. III/19. Berlin: Springer; 1994.
[2] Shen TD, Schwarz RB. Appl Phys Lett 1999;75:49.
[3] Pang S, Zhang T, Asami K, Inoue A. Mater Trans JIM 2002;43:2137.
[4] Chattoraj I, Baunack S, Stoica M, Gebert A. Mater Corr 2004;55:36.
[5] Inoue A. Bulk amorphous alloys. Uetikon-Zuerich Switzerland: Trans Tech Publications; 1999.
[6] Inoue A, Zhang W, Zhang T, Kurosaka K. Acta Mater 2001;49:2645.
[7] Inoue A. Acta Mater 2000;48:279.
[8] Inoue A, Shen BL, Yavari AR, Greer ALJ. Mater Res 2003;18:1487.
[9] Inoue A, Shen BL, Koshiba H, Kato H, Yavari AR. Acta Mater 2004; 52:1631.
[10] Inoue A, Wang XM. Acta Mater 2000;48:1383.
[11] Ponnambalam V, Poon SJ, Shiflet GJ. J Mater Res 2004;19:1320.
[12] Lu ZP, Liu CT, Thomson JR, Porter WD. Phys Rev Lett 2004;92: 245503.
[13] Stoica M, Eckert J, Roth S, Schultz L, Yavari AR, Kvick Å. J Metastable Nanocrystalline Mater 2002;12:77.
[14] Stoica M, Degmova J, Roth S, Eckert J, Grahl H, Schultz L, et al. Mater Trans 2002;43:1966.
[15] Stoica M, Eckert J, Roth S, Schultz L. Mater Sci Eng A 2004; 375–377:399.
[16] Chen HS. Rep Prog Phys 1980;43:353.
[17] Boll R. In: Siemens AG, editor. Weichmagnetische Werkstoffe, VAC GmbH. Germany: Berlin und München; 1990.
[18] Liu CT, Heatherly L, Easton DS, Carmichael CA, Schneibel JH, Chen CH, et al. Metall Mater Trans A 1998;29:1811.
[19] Zhang ZF, Eckert J, Schultz L. Acta Mater 2003;51:1167.
[20] Zhang ZF, He G, Eckert J, Schultz L. Phys Rev Lett 2003;91:045505.
[21] He G, Löser W, Eckert J, Schultz LJ. Mater Res 2002;17:3015.
[22] De Boer FR, Boom R, Mattens WCM, Miedema AR, Niessen AK. Cohesions in metals. Amsterdam, The Netherlands: North-Holland; 1988.